Ising model on three-dimensional random lattices: A Monte Carlo study

Wolfhard Janke[1] and Ramon Villanova[2]

[1]*Institut für Theoretische Physik, Universität Leipzig, Augustusplatz 10/11, 04109 Leipzig, Germany*
[2]*Matemàtica Aplicada, DEE, Universitat Pompeu Fabra, c/Ramon Trias Fargas, 25-27, 08005 Barcelona, Spain*

We report single-cluster Monte Carlo simulations of the Ising model on three-dimensional Poissonian random lattices with up to $128\,000 \approx 50^3$ sites which are linked together according to the Voronoi-Delaunay prescription. For each lattice size quenched averages are performed over 96 realizations. By using reweighting techniques and finite-size scaling analyses we investigate the critical properties of the model in the close vicinity of the phase transition point. Our random lattice data provide strong evidence that, for the available system sizes, the resulting effective critical exponents are indistinguishable from recent high-precision estimates obtained in Monte Carlo studies of the Ising model and ϕ^4 field theory on three-dimensional regular cubic lattices.

I. INTRODUCTION

Experimental studies of the critical behavior of real materials are often confronted with the influence of impurities and inhomogeneities. For a proper interpretation of the measurements it is, therefore, important to develop a firm theoretical understanding of the effect of such random perturbations. In many situations the typical time scale of thermal fluctuations in the idealized "pure" system is clearly separated from the time scale of the impurity dynamics, such that to a very good approximation the impurities can be treated as quenched (frozen), random disorder.

The importance of the effect of quenched, random disorder on the critical behavior of a physical system can be quite generally classified by the critical exponent of the specific heat of the pure system, α_p. The Harris criterion[1] asserts that for $\alpha_p > 0$ quenched, random disorder is a relevant perturbation, leading to a different critical behavior than in the pure case. In particular one expects[2] in the disordered system that $\nu \geq 2/D$, where ν is the correlation length exponent and D the dimension of the system. Assuming hyperscaling to be valid, this implies $\alpha = 2 - D\nu \leq 0$. For $\alpha_p < 0$ disorder is irrelevant, and in the marginal case $\alpha_p = 0$ no prediction can be made. For the case of (noncritical) first-order phase transitions it is known that the influence of quenched, random disorder can lead to a softening of the transition.[3]

Many theoretical and numerical studies have been devoted to quenched, random site-dilution (SD), bond-dilution (BD), or more general random-bond (RB) systems. Since for the three-dimensional (3D) Ising model it is well known that $\alpha_p \approx 0.1 > 0$, quenched, random disorder should be relevant for this model. This has indeed been verified by a variety of techniques: Monte Carlo (MC) simulations for SD (Refs. 4–6) and BD (Refs. 7 and 8), high-temperature series (HTS) expansions for BD (Ref. 9), and field theoretical renormalization group studies (Refs. 10–13). For an excellent review and an extensive list of experimental, theoretical, and numerical estimates in the last two decades, see Ref. 14. As a result consensus has been reached that, while the critical exponent ratios $\gamma/\nu = 2 - \eta$ and β/ν are hardly distinguishable from the pure model, the correlation length exponent ν

clearly signals the disordered fixed point,

$$\gamma/\nu = 1.966(6), \quad \beta/\nu = 0.517(3),$$

$$\nu = 0.6304(13) \quad \text{[pure (Ref. 15)]},$$

$$\gamma/\nu = 1.970(3), \quad \beta/\nu = 0.515(2),$$

$$\nu = 0.678(10) \quad \text{[disordered (Ref. 13)]},$$

and, moreover, satisfies the bound $\nu \geq 2/D = 2/3$ in the disordered case. Recently also the predicted softening effect at first-order phase transitions has been confirmed for 3D q-state Potts models with $q \geq 3$ using MC (Refs. 16–18) and HTS (Ref. 19) techniques.

The overall picture is even better in two dimensions where several models with $\alpha_p > 0$ (SD Baxter model,[20] SD Baxter-Wu model,[21], three- and four-state RB Potts model,[22] Ashkin-Teller model[23]) and the marginal ($\alpha_p = 0$) 2D Ising model[24–28] have been investigated. Also the softening of the first-order transitions for the 2D models with $q \geq 5$ has been confirmed.[29–32] For a recent review, see Ref. 33.

In this paper we study another type of quenched, random disorder: namely, *connectivity disorder*, a generic property of random lattices whose local coordination numbers vary randomly from site to site. Physically the concept of random lattices plays an important role in an idealized description of the statistical geometry of random packings of particles.[34–36] A prominent example is the crystallization process in liquids, and many statistical properties of random lattices have been studied in this context.[37] From a more technical point of view, random lattices provide a convenient tool to discretize spaces of nontrivial topology without introducing defects or any kind of anisotropy.[38–40] This desirable property has been exploited in a great variety of fields, ranging from diffusion limited aggregation[41] and growth models for sandpiles[42] over the statistical mechanics of membranes and strings[43] to quantum field theory and quantum gravity.[38–40,44,45] The preserved rotational, or more generally Poincaré, invariance suggests that spin systems or field theories defined on random lattices should reach the infinite-volume or continuum

limit faster than on regular lattices. Conceptually, however, such an approach only makes sense as long as the critical properties of the considered system are not modified by the irregular lattice structure. In view of the quite general Harris criterion this is a nontrivial question (in particular due to the inherent spatial correlations of the disorder in this case), at least for systems characterized by $\alpha_p \geqslant 0$.

Specifically we considered 3D Poissonian random lattices of Voronoi-Delaunay type and performed an extensive computer simulation study of the Ising model for lattices varying in size from $N = 2000 \approx 13^3$ to $128\,000 \approx 50^3$ sites. For each system size quenched averages over the connectivity disorder are approximated by averaging over 96 independent realizations. We concentrated on the close vicinity of the transition point and applied finite-size scaling (FSS) techniques[46] to extract the critical exponents and the (weakly universal) "renormalized charges" U_2^* and U_4^*. To achieve the desired accuracy of the data in reasonable computer time we applied the single-cluster algorithm[47,48] to update the spins and furthermore made extensively use of the reweighting technique.[49]

Previous studies of connectivity disorder focused mainly on 2D where pronounced effects were observed in MC simulations of q-state Potts models on quenched, random graphs provided by models of quantum gravity [modified universality classes for $q = 2$ and 4 (Refs. 50–52), and softening for $q = 10$ (Refs. 52 and 53)]. For 2D random lattices of Voronoi-Delaunay type, on the other hand, no influence was seen in simulations for $q = 2$ (Refs. 54 and 55) and $q = 8$ (Ref. 56). The main difference between these two types of random lattices is the highly fractal structure[57] of random gravity graphs which suggests a stronger "degree of disorder." A similar dependence on the "degree of disorder" was recently observed for several aperiodic perturbations.[58]

The rest of the paper is organized as follows. In Sec. II, we describe some properties of the random lattices used in the simulations, and in Sec. III we define the model and give a few simulation details including estimates of autocorrelation times. The quantities measured are defined in Sec. IV, where also their theoretically expected FSS behavior is recalled. In Sec. V, we present the FSS analysis of our data close to the transition point which yields estimates for the critical exponents. Finally, in Sec. VI we present a discussion of our main results and close with a few concluding remarks.

II. RANDOM LATTICES

A. Voronoi-Delaunay random lattices

The notion of a "random lattice" is by no means unique and, in fact, many different types of random lattices have been considered in the recent literature.[41,50,52,53,59] In this paper we concentrate on so-called Poissonian Voronoi-Delaunay random lattices which, in arbitrary dimensions, are defined as follows.[38,44,45]

(i) Draw N sites x_i at random in a unit volume (square in 2D, cube in 3D, ...).

(ii) Associate with each site x_i a Voronoi cell, $c_i \equiv \{x | d(x, x_i) \leqslant d(x, x_j) \quad \forall j \neq i\}$, which consists of all points x that are closer to the center site x_i than to any other site.

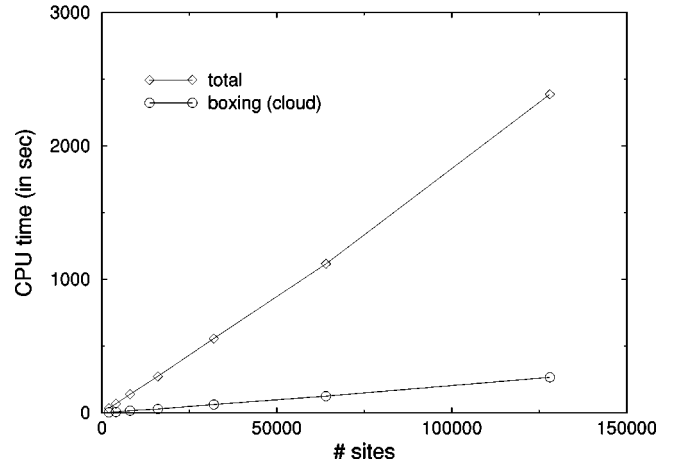3D Poissonian Voronoi/Delaunay random lattices

FIG. 1. The total CPU time spent in constructing a three-dimensional Poissonian random lattice according to the Voronoi-Delaunay prescription vs the number of sites N. The circles show the fraction of time needed to set up the "cloud of neighbors" discussed in the Appendix.

Here $d(x, y)$ denotes the usual Euclidean distance. This yields an irregular tessellation of the unit volume with D-dimensional Voronoi cells (polygons in 2D, polyhedra in 3D, ...).

(iii) Construct the dual Delaunay lattice by linking the center sites of all Voronoi cells which share a common face.

The first step approximates the Poissonian process. In the second step we always assume periodic boundary conditions, i.e., construct lattices of toroidal topology. Using this construction the number of nearest neighbors of the Delaunay lattice, the *local* coordination number q, varies randomly from site to site. This constitutes the special type of quenched, random connectivity disorder we are investigating in this work.

The actually employed construction of the random lattices follows loosely the method of Ref. 60 and is described in the Appendix. Following this method we succeeded to reduce the complexity of the lattice construction for all practical purposes from order N^2, as expected for the most straightforward implementation, to order N, up to a small overhead $\propto N^2$ resulting from the initial calculation of the distances between all pairs of two sites. The actually measured CPU times as a function of N are shown in Fig. 1.

B. Random lattice properties

To test our random lattice construction we measured several quantities which characterize the topology and geometry of the lattices. These quantities are exactly known in the limit $N \to \infty$. "Topological" quantities are the number of links N_l, the number of triangles $N_\triangle$, and the number of tetrahedra N_τ, which according to Euler's theorem should satisfy for a torus topology in any number of dimensions and for *any* number of sites N the relation

$$N - N_l + N_\triangle - N_\tau = 0. \qquad (1)$$

TABLE I. The average coordination number $\bar{q}$ and the total number of simplices normalized by the number of sites. The error bars are computed from the fluctuations among the 96 realizations.

N	$\bar{q}$	N_l/N	$N_\triangle/N$	N_τ/N
2 000	15.544(4)	7.7721(19)	13.5441(37)	6.7721(19)
4 000	15.532(3)	7.7661(16)	13.5321(32)	6.7661(16)
8 000	15.537(2)	7.7683(10)	13.5366(21)	6.7683(10)
16 000	15.535(2)	7.76 744(76)	13.5348(15)	6.76744(76)
32 000	15.534(1)	7.76 706(55)	13.5342(11)	6.76706(55)
64 000	15.5351(7)	7.76 755(36)	13.53507(72)	6.76755(36)
128 000	15.5349(5)	7.76 743(26)	13.53486(53)	6.76743(26)
Exact	15.5354 . . .	7.76 772 . . .	13.53545 . . .	6.76772 . . .
Exact	$2+\dfrac{48}{35}\pi^2$	$1+\dfrac{24}{35}\pi^2$	$\dfrac{48}{35}\pi^2$	$\dfrac{24}{35}\pi^2$

We have of course explicitly tested that this topological constraint is satisfied for all realizations, which is quite a sensitive confirmation that the lattice construction works properly. The measured averages of q, N_l, $N_\triangle$, and N_τ over the 96 realizations used in the simulations are collected in Table I. The error bars are computed from the fluctuations among the 96 realizations. We see that the analytically known $N\rightarrow\infty$ limits are approached very rapidly. The only exception is perhaps our smallest lattice with $N=2000$ sites where deviations from the infinite-volume limit are clearly visible. For $N\geq4000$ in particular the average number of nearest neighbors, $\bar{q}$, is fully consistent with the theoretical value of

$$\bar{q}=2+\frac{48}{35}\pi^2=15.5354 \ldots . \qquad (2)$$

As "geometric" quantities we measured the average volumes of the simplices, i.e., the average link length $\bar{l}=\Sigma_{i=1}^{N_\tau}[(\Sigma_{i\in\tau}l_i)/6]/N_\tau$, the average triangle area $\bar{\triangle}=(\Sigma_{i=1}^{N_\triangle}\triangle_i)/N_\triangle$, and the average volume of a tetrahedron $\bar{\tau}=(\Sigma_{i=1}^{N_\tau}\tau_i)/N_\tau$. Notice that the average link length is de-

fined in such a way that we first average over the sides of a given tetrahedron and then over all the tetrahedra. This is thus the average link length per tetrahedron, and *not* the mean link length averaged over the whole lattice, $\bar{l}^{(N)}=(\Sigma_{i=1}^{N_l}l_i)/N_l$, which is always larger due to the fluctuations in the number of tetrahedra from realization to realization. Our results normalized with an appropriate power of the density $\rho=N/V$ are displayed in Table II. From $N=4000$ on the numerical results are again fully consistent with the analytical predictions as $N\rightarrow\infty$. Since all numbers agree very well with the analytical predictions, we can be quite sure that our lattice construction works properly and that we have picked a typical sample of random lattices.

The (normalized) probability densities $P(q)$ of the coordination numbers q are shown in Fig. 2 for the lattices with $N=64000$ and $N=128000$ sites. The average coordination number is $\bar{q}=2+\frac{48}{35}\pi^2=15.5354 \ldots$. Due to the long tail of $P(q)$ for large values of q, the maximum of $P(q)$ is found at the next smaller integer number $q=15$, which occurs with a probability of 12.03%.

III. MODEL AND SIMULATION TECHNIQUES

A. Model

We simulated the standard partition function of the Ising model,

$$Z=\sum_{\{s_i\}}e^{-KE}, \quad E=-\sum_{\langle ij\rangle}s_is_j, \quad s_i=\pm1, \qquad (3)$$

where $K=J/k_BT>0$ is the inverse temperature in natural units and $\langle ij\rangle$ denotes the nearest-neighbor links of our three-dimensional toroidal random lattices. In Eq. (3) we have adopted the convention used in Ref. 55 and assigned to each link the same weight.

Another interesting option would be to assign to each link a weight depending on the geometrical properties of the Voronoi-Delaunay construction such as the length of the links or suitably defined areas of the associated tesselation. In addition to the connectivity disorder this would introduce also a (correlated) disorder of random-bond type. In order

TABLE II. Average simplex volumes properly normalized to natural units.

| N	$\bar{l}^{(N)}/\rho^{-1/3}$	$\bar{l}/\rho^{-1/3}$	$\bar{\triangle}/\rho^{-2/3}$	$\bar{\tau}/\rho^{-1}$
2 000	1.28540(22)	1.236 70(17)	0.597 004(95)	0.147 666(41)
4 000	1.28566(18)	1.237 17(13)	0.597 362(70)	0.147 797(34)
8 000	1.28569(13)	1.237 11(10)	0.597 312(55)	0.147 747(23)
16 000	1.285623(75)	1.237 091(55)	0.597 306(31)	0.147 766(17)
32 000	1.285554(68)	1.237 027(49)	0.597 289(24)	0.147 775(12)
64 000	1.285537(40)	1.237 002(32)	0.597 272(19)	0.147 7630(78)
128 000	1.285541(28)	1.237 012(20)	0.597 275(11)	0.147 7666(58)
Exact		1.237 033 . . .	0.597 286 . . .	0.147 7600 . . .
Exact		$\left(\dfrac{3}{4\pi}\right)^{1/3}\dfrac{5\times7^3}{3^2\times4^4}\Gamma\left(\dfrac{1}{3}\right)$	$\left(\dfrac{3}{4\pi}\right)^{2/3}\dfrac{5^3\times7}{3^5\pi}\Gamma\left(\dfrac{2}{3}\right)$	$\dfrac{35}{24\pi^2}$
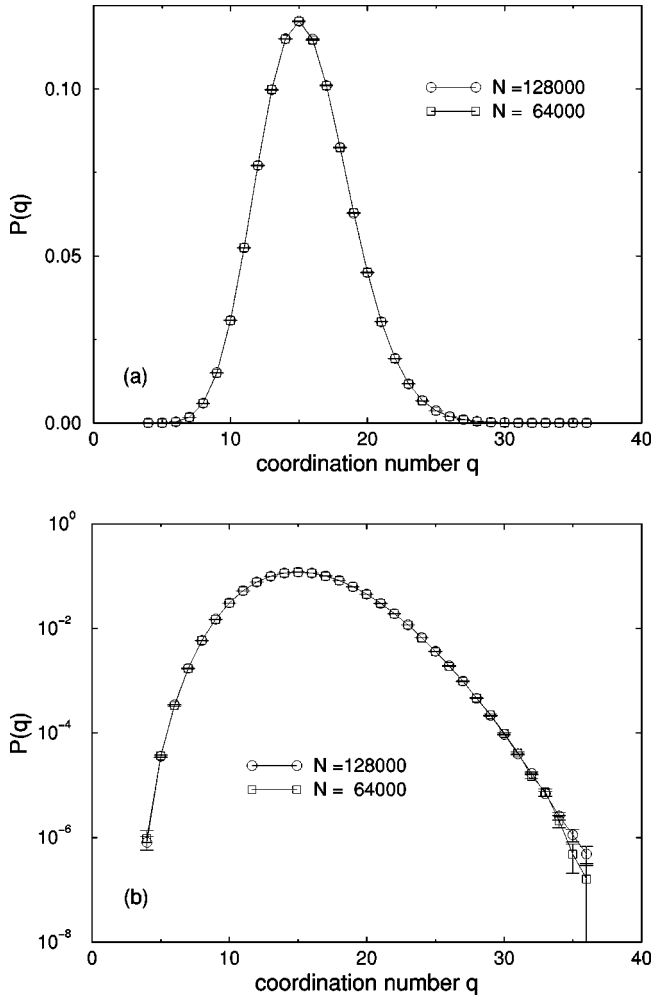
FIG. 2. (a) The probability density $P(q)$ of the coordination numbers q. The average is $\bar{q} = 2 + 48\pi^2/35 = 15.5354\ldots$. (b) The same data as in (a) on a logarithmic scale.

not to mix up these two quenched disorder types, we decided to concentrate in this study exclusively on the effect of the connectivity disorder.

B. Simulation

The finite-size scaling analysis is performed on the basis of seven different lattice sizes with $N = 2000$, 4000, 8000, 16 000, 32 000, 64 000, and 128 000 sites. For later use we adopt the notation for regular lattices and define a linear lattice size L by $L = N^{1/3}$. The linear sizes of the lattices thus vary from $L \approx 12.6$ to $L \approx 50.4$. To investigate the dependence of thermal averages on different realizations we performed MC simulations, for each lattice size, on the 96 randomly chosen random lattice realizations discussed in Sec. II.

For the update of the Ising spins we employed Wolff's single-cluster (1C) algorithm.[47] Various tests, in particular for the Ising model on two- and three-dimensional regular lattices, have clearly demonstrated that critical slowing down can be significantly reduced with this nonlocal update algorithm.[61–63] These tests also showed that in particular in

three dimensions the single-cluster algorithm is more efficient than the original multiple-cluster formulation of Swendsen and Wang.[48]

All runs were performed in the vicinity of the critical point K_c. As a first rough guess of K_c we used the mean-field bound $K_c \geq K_{MF} = 1/\bar{q} \approx 0.064$. Due to the large average coordination number of 3D random lattices, the mean-field approximation should be better than for the simple cubic (SC) lattice where $K_{MF}^{(SC)} = 1/6$ is about 1.33 times smaller than the actual $K_c^{(SC)} \approx 0.221\,654\,6$. Therefore, by applying the same correction factor to the random lattice mean-field estimate we expect that K_c is bounded from above by $K_c \leq 0.085$. This heuristic argument thus suggests that $0.064 \leq K_c \leq 0.085$, such that $K_c \approx 0.075$ should be a reasonable *a priori* guess. Once good simulation points K_0 were estimated for the two smallest lattices with $N = 2000$ and 4000 sites by determining for a few realizations the location of the specific-heat and susceptibility maxima, we used FSS extrapolations (assuming $\nu \approx 0.63$) to predict K_0 for the larger lattices.

Depending on the lattice size from 30 000 to 180 000 clusters were discarded to reach equilibrium from an initially completely ordered state. Primary observables are the energy per spin, $e = E/N$, and the magnetization per spin, $m = M/N = \Sigma_i s_i/N$, which were measured every n_{flip} cluster flip and recorded in a time-series file. The average cluster size $\langle |C| \rangle$ is an estimator for the reduced susceptibility in the high-temperature phase, $\chi_{red} = N\langle m^2 \rangle$, and therefore scales with the lattice size according to $L^{\gamma/\nu}$, where γ and ν are the usual critical exponents. Since in three dimensions $\gamma/\nu = 2 - \eta \approx 2$, we have to perform $n_{flip} \propto L$ cluster flips in order to flip, on the average, approximately the same fraction of the total number of spins, $N = L^3$, for all lattice sizes. By adjusting the absolute scale of n_{flip} we made sure that for all lattice sizes the measurements were taken after about $N/2$ spin flips. Since for the single-cluster update algorithm the autocorrelation times scale only weakly with L (see the discussion below) one then expects that, with about the same number of measurements, the statistical accuracy is comparable for all lattice sizes. With this setup we performed 100 000 measurements for each lattice size and realization (110 000 for $N = 8000$). For more details on the employed statistics, see Table III.

C. Update dynamics

A useful measure of the update dynamics is the integrated autocorrelation time $\hat{\tau}$.[64] To estimate $\hat{\tau}$ for the measurements of the energy e and the magnetization m we used the fact that $\hat{\tau}$ enters in the error estimate $\epsilon^2 = \sigma^2 2\hat{\tau}/n_{meas}$ for the mean value $\bar{O}$ of n_{meas} correlated measurements with variance $\sigma^2 = \langle O; O \rangle \equiv \langle O^2 \rangle - \langle O \rangle^2$ and determined ϵ^2 by blocking procedures. Using 100 blocks of 1000 measurements each we obtained the results compiled in Table IV where all results are averaged over the 96 randomly chosen realizations. We see that the integrated autocorrelation times for the measurements of e and m are of the order of $\hat{\tau}_e \approx 2.5$–3.5 and $\hat{\tau}_m \approx 2.4$–3.0. Since completely uncorrelated data correspond to

TABLE III. Monte Carlo parameters of the simulations. $N \equiv L^3$ is the lattice size, the hash mark symbol # denotes the number of realizations, K_0 the inverse simulation temperature, n_{therm} the number of cluster flips during equilibration, and n_{meas} the number of measurements taken every n_{flip} cluster flip.

N	L	#	K_0	n_{therm}	n_{meas}	n_{flip}
2 000	12.6	96	0.0735	30 000	100 000	4
4 000	15.9	96	0.0735	50 000	100 000	5
8 000	20.0	96	0.0732	66 000	110 000	6
16 000	25.2	96	0.0729	80 000	100 000	8
32 000	31.7	96	0.072 85	100 000	100 000	10
64 000	39.1	96	0.072 65	150 000	100 000	13
128 000	50.4	32	0.072 53	180 000	100 000	16
128 000	50.4	64	0.072 59	180 000	100 000	16

$\hat{\tau} = 0.5$, our thermal sample thus effectively consists of about 15 000–20 000 uncorrelated measurements for each of the 96 realizations. This amounts to a total of $(1.5–2.0) \times 10^6$ effectively uncorrelated measurements for each lattice size.

While this properly characterizes the effective statistics of our simulations, the numbers for $\hat{\tau}$ of a single-cluster simulation are not yet well suited for a comparison with other update algorithms or with single-cluster simulations on regular lattices. To get a comparative work estimate, the usual procedure[47] is to convert the $\hat{\tau}$ by multiplying by a factor $f = n_{\text{flip}}\langle|C|\rangle/N$ to a scale where, on the average, measurements are taken after every spin has been flipped once (similar to, e.g., Metropolis simulations). For quenched, random systems this procedure is not unique due to the necessary average over realizations. In Table IV we therefore present both options $[\tau]_{\text{av}} \equiv [f \cdot \hat{\tau}]_{\text{av}}$ and also $[f]_{\text{av}} \cdot [\hat{\tau}]_{\text{av}}$. The differences between the two averaging prescriptions are, however, extremely small.

The numbers in Table IV obtained in this way are very similar to results for the regular SC lattice.[61,62] By fitting a power law $\tau \propto L^z$ to the data for the five largest lattices we obtain $[\tau_e]_{\text{av}} = 0.82(6)L^{0.20(2)}$ and $[\tau_m]_{\text{av}} = 1.07(8)L^{0.10(2)}$, respectively. The dynamic critical exponents z for the random lattice simulations should be compared with $z_e = 0.28(2)$ and $z_\chi = 0.14(2)$ for the SC lattice.[61]

IV. OBSERVABLES AND FINITE-SIZE SCALING

From the time series of e and m it is straightforward to compute in the FSS region various quantities at nearby values of K_0 by standard reweighting methods.[49] For the estimation of the statistical (thermal) errors, for each of the 96 realizations the time-series data were split into 100 bins, which were jackknifed[65] to decrease the bias in the analysis of reweighted data. The final values are averages over the 96 realizations which will be denoted by square brackets $[\cdots]_{\text{av}}$, and the error bars are computed from the fluctuations among the realizations. Note that these errors contain both the average thermal error for a given realization and the theoretical variance for infinitely accurate thermal averages which is caused by the variation of the quenched, random geometry of the 96 lattices.

From the time series of the energy measurements we can compute by reweighting the average energy, specific heat, and energetic fourth-order parameter:

$$u(K) = [\langle E \rangle]_{\text{av}}/N, \tag{4}$$

$$C(K) = K^2 N [\langle e^2 \rangle - \langle e \rangle^2]_{\text{av}}, \tag{5}$$

$$V(K) = \left[1 - \frac{\langle e^4 \rangle}{3\langle e^2 \rangle^2} \right]_{\text{av}}. \tag{6}$$

Similarly we can derive from the magnetization measurements the average magnetization, the susceptibility, and the magnetic cumulants:

$$m(K) = [\langle |m| \rangle]_{\text{av}}, \tag{7}$$

$$\chi(K) = K N [\langle m^2 \rangle - \langle |m| \rangle^2]_{\text{av}}, \tag{8}$$

$$U_2(K) = \left[1 - \frac{\langle m^2 \rangle}{3\langle |m| \rangle^2} \right]_{\text{av}}, \tag{9}$$

$$U_4(K) = \left[1 - \frac{\langle m^4 \rangle}{3\langle m^2 \rangle^2} \right]_{\text{av}}. \tag{10}$$

Further useful quantities involving both the energy and magnetization are

TABLE IV. Average cluster size $[\langle|C|\rangle]_{\text{av}}$ and autocorrelation times of energy and magnetization at the simulation point K_0, where $\tau = f \cdot \hat{\tau}$ and $f = n_{\text{flip}}\langle|C|\rangle/N$. The tau's are obtained from a blocking analysis on the basis of 100 block.

N	$[\langle|C|\rangle]_{\text{av}}$	$[\hat{\tau}_e]_{\text{av}}$	$[\tau_e]_{\text{av}}$	$[f]_{\text{av}} \cdot [\hat{\tau}_e]_{\text{av}}$	$[\hat{\tau}_m]_{\text{av}}$	$[\tau_m]_{\text{av}}$	$[f]_{\text{av}} \cdot [\hat{\tau}_m]_{\text{av}}$
2 000	246.9(1.9)	2.529(40)	1.245(19)	1.249	2.434(38)	1.200(20)	1.202
4 000	453.3(3.9)	2.443(42)	1.375(20)	1.384	2.412(38)	1.360(20)	1.367
8 000	740.1(5.5)	2.702(42)	1.494(22)	1.500	2.594(40)	1.436(22)	1.440
16 000	1084.0(9.5)	2.955(43)	1.593(21)	1.602	2.730(38)	1.475(22)	1.480
32 000	1962(17)	2.741(50)	1.666(24)	1.681	2.572(44)	1.567(23)	1.577
64 000	2678(24)	3.177(55)	1.718(27)	1.728	2.795(42)	1.516(23)	1.520
128 000	3521(87)	3.92(11)	1.705(42)	1.725	3.157(72)	1.385(42)	1.390
128 000	4325(41)	3.399(72)	1.824(31)	1.838	2.964(60)	1.593(29)	1.602

$$\frac{d[\langle|m|\rangle]_{\mathrm{av}}}{dK}=[\langle|m|E\rangle-\langle|m|\rangle\langle E\rangle]_{\mathrm{av}}, \qquad (11)$$

$$\frac{d\ln[\langle|m|\rangle]_{\mathrm{av}}}{dK}=\left[\frac{\langle|m|E\rangle}{\langle|m|\rangle}-\langle E\rangle\right]_{\mathrm{av}}, \qquad (12)$$

$$\frac{d\ln[\langle m^2\rangle]_{\mathrm{av}}}{dK}=\left[\frac{\langle m^2 E\rangle}{\langle m^2\rangle}-\langle E\rangle\right]_{\mathrm{av}}. \qquad (13)$$

In the infinite-volume limit these quantities exhibit singularities at the transition point. In finite systems the singularities are smeared out and scale in the critical region according to

$$C=C_{\mathrm{reg}}+L^{\alpha/\nu}f_C(x)[1+\cdots], \qquad (14)$$

$$[\langle|m|\rangle]_{\mathrm{av}}=L^{-\beta/\nu}f_m(x)[1+\cdots], \qquad (15)$$

$$\chi=L^{\gamma/\nu}f_\chi(x)[1+\cdots], \qquad (16)$$

$$\frac{d[\langle|m|\rangle]_{\mathrm{av}}}{dK}=L^{(1-\beta)/\nu}f_{m'}(x)[1+\cdots], \qquad (17)$$

$$\frac{d\ln[\langle|m|^p\rangle]_{\mathrm{av}}}{dK}=L^{1/\nu}f_p(x)[1+\cdots], \qquad (18)$$

$$\frac{dU_{2p}}{dK}=L^{1/\nu}f_{U_{2p}}(x)[1+\cdots], \qquad (19)$$

where C_{reg} is a regular background term, ν, α, β, and γ, are the usual critical exponents, $f_i(x)$ are FSS functions with

$$x=(K-K_c)L^{1/\nu} \qquad (20)$$

being the scaling variable, and the brackets $[1+\cdots]$ indicate corrections-to-scaling terms which become unimportant for sufficiently large system sizes L.

V. RESULTS

By applying standard reweighting techniques to each of the 96 time-series data we first determined the temperature dependence of $C_i(K)$, $\chi_i(K)$, ..., $i=1,\ldots,96$, in the neighborhood of the simulation point K_0. By estimating the valid reweighting range for each of the realizations we made sure that no systematic errors crept in by this procedure. Once the temperature dependence is known for each realization, we can easily compute the disorder average, e.g., $C(K)=\Sigma_{i=1}^{96}C_i(K)/96$, and then determine the maxima of the averaged quantities, e.g., $C_{\max}(K_{\max_C})\equiv\max_K C(K)$. The locations of the maxima of C, χ, dU_2/dK, dU_4/dK, $d[\langle|m|\rangle]_{\mathrm{av}}/dK$, $d\ln[\langle|m|\rangle]_{\mathrm{av}}/dK$, and $d\ln[\langle m^2\rangle]_{\mathrm{av}}/dK$ provide us with seven sequences of pseudotransition points $K_{\max_i}(L)$ which all should scale according to $K_{\max_i}(L)=K_c+a_iL^{-1/\nu}+\cdots$. In other words, the scaling variable $x=(K_{\max_i}(L)-K_c)L^{1/\nu}=a_i+\cdots$ should be constant if we neglect the small higher-order corrections indicated by the ellipsis. To give an idea on how these sequences approach K_c

TABLE V. Fit results for the critical coupling K_c, using the FSS ansatz $K_{\max_i}=K_c+a_iL^{-1/\nu}$ and our best estimate of $1/\nu=1.5875(12)$. The fit range is always from $N=4000$ to $128\,000$.

$K_{\max}$ of	K_c	a	Q
C	0.072 428 2(40)	0.1010(12)	0.63
χ	0.072 421 0(40)	0.0182(11)	0.87
dU_4/dK	0.072 422 1(54)	−0.0326(14)	0.65
dU_2/dK	0.072 423 8(44)	0.0002(12)	0.89
$d[\langle|m|\rangle]_{\mathrm{av}}/dK$	0.072 427 7(40)	0.0525(11)	0.82
$d\ln[\langle|m|\rangle]_{\mathrm{av}}/dK$	0.072 425 0(43)	−0.0063(12)	0.83
$d\ln[\langle m^2\rangle]_{\mathrm{av}}/dK$	0.072 4 253(44)	−0.0146(12)	0.76
Average	0.072 424 7(10)		
Weighted av.	0.072 424 9(16)		
Final	0.072424 9(40)		

we show in Table V besides the estimates for K_c also the values of a_i, $i=1,\ldots,7$ (see also Fig. 4).

It should be emphasized that while the precise estimates of a_i do depend on the value of ν, the qualitative conclusion that $x\approx$const for $K_{\max_i}$ does not require any *a priori* knowledge of ν or K_c. Using this information we have thus several possibilities to extract unbiased estimates of the critical exponents ν, α/ν, β/ν, and γ/ν from least-squares fits assuming the FSS behaviors (14)–(19). Once ν is estimated we can then use $K_{\max_i}(L)=K_c+a_iL^{-1/\nu}+\cdots$ to extract also K_c and a_i.

A. Critical exponent ν

Let us thus start with the correlation length exponent ν for which we can obtain $4\times7=28$ different estimates by considering the scaling of $d\ln[\langle|m|\rangle]_{\mathrm{av}}/dK$, $d\ln[\langle m^2\rangle]_{\mathrm{av}}/dK$, dU_2/dK, and dU_4/dK at the seven sequences of pseudo-transition points $K_{\max_i}(L)$. Of course, these estimates are statistically *not* uncorrelated, but they are differently affected by corrections to the leading FSS behavior. To test the importance of these corrections to scaling we first estimated ν from fits using all available lattice sizes and then compared with the results of fits where the two smallest sizes were successively discarded. As a result we did not observe any systematic improvement by omitting the smallest lattices. In fact, already for the fits using all sizes, we obtained goodness-of-fit parameters[66] $Q\geq0.3$ for about 80% of the 28 fits. The only unacceptable fit was that of $d\ln[\langle m^2\rangle]_{\mathrm{av}}/dK$ at the $K_{\max_\chi}$ sequence with $Q=0.01$. Here we omitted the $N=2000$ data point which improves the goodness to $Q=0.22$.
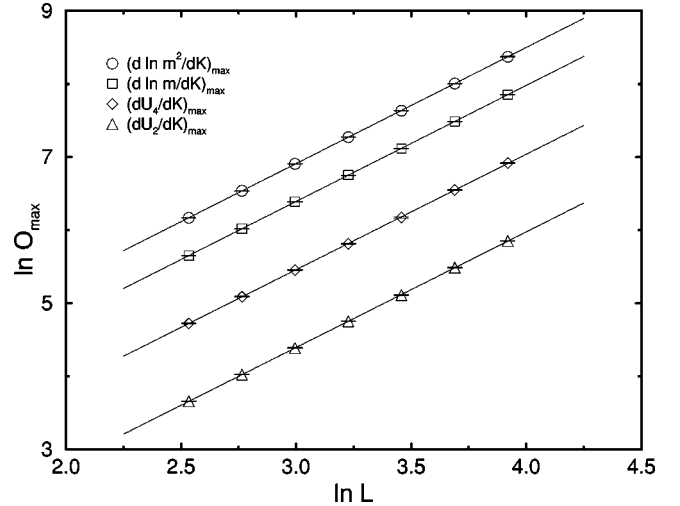
This analysis clearly shows that with our data there is no need to include corrections-to-scaling terms in the fits which would necessitate nonlinear fitting procedures which usually tend to be quite unstable. Of course, such a conclusion depends on the accuracy of the data and only shows that the correction terms are so small that they cannot be resolved within our accuracy. This is quite remarkable because in the pure 3D Ising model study of Ref. 67 for lattices of size L

TABLE VI. Fit results for the critical exponent $1/\nu$.

Quantity	Type	$1/\nu$
dU_2/dK	at maximum	1.5818(33)
	average	1.5783(32)
	weighted av.	1.5795(12)
	final	1.5795(27)
dU_4/dK	at maximum	1.5797(42)
	average	1.5763(34)
	weighted av.	1.5774(13)
	final	1.5774(25)
dU_{2p}/dK	average	1.5773(23)
$p=1$ and 2	weighted av.	1.5785(09)
	final	1.5785(25)
$d\ln[\langle|m|\rangle]_{av}/dK$	at maximum	1.5886(16)
	average	1.5888(08)
	weighted av.	1.5889(06)
	final	1.5889(14)
$d\ln[\langle m^2\rangle]_{av}/dK$	at maximum	1.5894(15)
	average	1.5902(07)
	weighted av.	1.5898(06)
	final	1.5898(12)
$d\ln[\langle m^p\rangle]_{av}/dK$	average	1.5895(06)
$p=1$ and 2	weighted av.	1.5894(05)
	final	1.5894(12)
$(dU_{2p}/dK)_{max}$ and	average	1.5849(25)
$(d\ln[\langle m^p\rangle]_{av}/dK)_{max}$	weighted av.	1.5878(10)
(4 fits)	final	1.5878(15)
dU_{2p}/dK and	average	1.5834(16)
$d\ln[\langle m^p\rangle]_{av}/dK$	weighted av.	1.5875(04)
(28 fits)	final	1.5875(12)

FIG. 3. FSS fits to extract $1/\nu$.

tion that the error of the weighted average is never larger than the error of the most accurate fit result that contributes to this average). As a general trend we see in Table VI that the fits of $d\ln[\langle|m|^p\rangle]_{av}/dK$ yield more accurate results than those of dU_{2p}/dK. We also observe, however, that the partial averages over the fits of dU_{2p}/dK, $p=1,2$ and $d\ln[\langle|m|^p\rangle]_{av}/dK$, $p=1,2$ are only marginally consistent, even though in all cases the goodness of fit was high. We thus have no reason based on statistical arguments to favor one or the other group of fits and therefore take as our final value the weighted average over all 28 estimates which yields

$$1/\nu = 1.5875 \pm 0.0012, \qquad \nu = 0.62992 \pm 0.00048, \quad (21)$$

with the minimal error coming from the fit of $d\ln[\langle|m|^2\rangle]_{av}/dK$ at the maximum locations of $d[\langle|m|\rangle]_{av}/dK$.

If we only average the results of the fits of the maxima of $d\ln[\langle|m|\rangle]_{av}/dK$, $d\ln[\langle m^2\rangle]_{av}/dK$, dU_2/dK, and dU_4/dK, we obtain basically the same final estimate with a slightly larger error bar:

$$1/\nu = 1.5878 \pm 0.0015, \quad \nu = 0.62980 \pm 0.00060. \quad (22)$$

To give also a visual impression of the quality of these fits, they are shown in Fig. 3. This reconfirms the weighted average (21) over all 28 fits, and our final estimate for the correlation length exponent is thus

$$\nu = 0.6299 \pm 0.0005. \qquad (23)$$

For comparison, for Ising models on regular SC lattices Ferrenberg and Landau[68] obtained $\nu=0.6289(8)$, Blöte *et al.*[69] concluded that $\nu=0.6301(8)$, Ballesteros *et al.*[67] found[70] $\nu=0.6294(5)[5]$, and in a recent study of the ϕ^4 lattice field theory Hasenbusch[71] estimated $\nu=0.6296(3)[4]$. Within error bars all three estimates are in perfect agreement with our result (23) for random lattices.

$=8$–128 (using a different FSS technique) confluent corrections to scaling $\propto L^{-\omega}$ with $\omega=0.87(9)$ could be resolved. One possible explanation is that random lattices with large average coordination number and preserved rotational invariance indeed reach the infinite-volume limit earlier than their regular counterparts. This is quite conceivable since the magnitude of the correction term does not only depend on the exponent but also on its amplitude, and the latter is a non-universal quantity which does definitely depend on the lattice structure.

Having now 28 estimates of $1/\nu$ from fits with $Q \geqslant 0.15$ we proceeded as follows. We computed arithmetic and error weighted averages for the four subgroups of estimates and finally over the total set of estimates. The main results are collected in Table VI. Because of the neglected cross correlations between the fit results, in particular the error estimate of the weighted average should be taken with some care. As our best estimates we therefore quote throughout this paper in all tables in the lines labeled ''final'' always the weighted mean and quite conservatively the smallest error among all available fits (making thus the plausible assump-
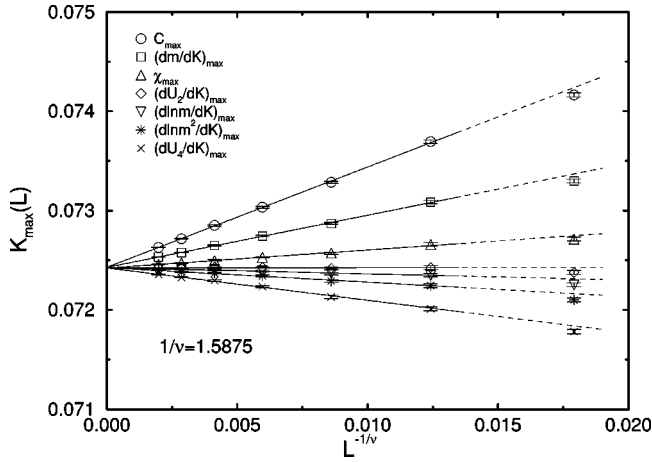
FIG. 4. FSS fits of the pseudotransition points $K_{\max_i}$ with $1/\nu = 1.5875$ fixed, yielding a combined estimate of $K_c = 0.072\,424\,9(40)$.

B. Critical coupling K_c

Having determined the critical exponent ν, it is straightforward to obtain estimates of the critical coupling K_c from linear least-squares fits to

$$K_{\max_i} = K_c + a_i L^{-1/\nu}, \qquad (24)$$

where $K_{\max_i}$ are the seven pseudotransition points discussed earlier. Here we found a significant improvement of the quality of the fits if the smallest lattice size with $N = 2000$ was excluded. This can also be inspected visually in Fig. 4, where the data and fits are shown. We see a systematic trend that the $N = 2000$ data lie a little bit too low. In Table V we therefore display the fit results over the six lattice sizes $N = 4000 - 128\,000$. By using the same averaging procedure as before we arrive at the final estimate

$$K_c = 0.072\,424\,9 \pm 0.000\,004\,0. \qquad (25)$$

Of course, in principle this estimate is biased by our estimate of ν. We have checked, however, that the dependence on ν is extremely weak. If we repeat the fits with $1/\nu = 1.5875$

$\pm 3\epsilon_{1/\nu}$, where $\epsilon_{1/\nu} = 0.0012$ is the error on the estimate of $1/\nu$ in Eq. (21), we obtain a variation in the estimate for K_c by only ± 2 in the last digit, which is much smaller than the statistical error in Eq. (25).

C. Critical exponent γ

The exponent ratio γ/ν can be obtained from fits to the FSS behavior (16) of the susceptibility. By monitoring the quality of the fits we decided to discard the $N = 2000$ data for the $K_{\max_C}$ and $K_{\max_{dm/dK}}$ sequences (which led to Q values of 0.05 and 0.02, respectively). The fits collected in Table VII then all have $Q \geqslant 0.25$. The final result is

$$\gamma/\nu = 1.9576 \pm 0.0013, \qquad (26)$$

which should be compared with the estimates for regular SC lattices of $\gamma/\nu = 1.970(14)$ in Ref. 68, $\gamma/\nu = 1.9630(30)$ in Ref. 69, $\gamma/\nu = 1.9626(6)[6]$ in Ref. 67, and $\gamma/\nu = 1.9642(4)[5]$ in Ref. 71.[70]

For the exponent η, the estimate (26) implies

$$\eta = 2 - \gamma/\nu = 0.0424 \pm 0.0013, \qquad (27)$$

and, by using our value (21) for $1/\nu$, we derive

$$\gamma = 1.2332 \pm 0.0018. \qquad (28)$$

D. Critical exponent β

The exponent ratio β/ν can be either obtained from the FSS behavior of $[\langle |m| \rangle]_{av}$ or $d[\langle |m| \rangle]_{av}/dK$, Eq. (15) or (17). In the first case, the sequences $K_{\max_\chi}$ and $K_{\max_{dm/dK}}$ yield poor Q values ($\leqslant 0.01$) if the $N = 2000$ are included in the fits. If we discard the smallest lattice in these two cases, all fits shown in Table VII are characterized by $Q \geqslant 0.10$. The final estimate is then

$$\beta/\nu = 0.51587 \pm 0.00082, \qquad (29)$$

and, by using our estimate for $1/\nu$ in Eq. (21),

$$\beta = 0.32498 \pm 0.00077. \qquad (30)$$

TABLE VII. Fit results for the critical exponents γ/ν, β/ν, and $(1-\beta)/\nu$. The superscripts * and # at the Q values indicate that these fits start at $N = 4000$ and $N = 8000$, respectively. The other fits use all data from $N = 2000$ to $128\,000$.

| $K_{\max}$ of	γ/ν	Q	β/ν	Q	$(1-\beta)/\nu$	Q
C	1.9357(37)	0.49*	0.5089(11)	0.10	1.0690(32)	0.82#
χ	1.9551(13)	0.36	0.523 74(82)	0.85*	1.0663(14)	0.30
dU_4/dK	1.9641(25)	0.35	0.5180(41)	0.27	1.0707(39)	0.20
dU_2/dK	1.9581(13)	0.59	0.5173(22)	0.31	1.0713(19)	0.15
$d[\langle |m| \rangle]_{av}/dK$	1.9476(19)	0.29*	0.510 97(95)	0.10*	1.0683(24)	0.65#
$d \ln[\langle |m| \rangle]_{av}/dK$	1.9603(13)	0.76	0.5140(19)	0.28	1.0657(29)	0.90#
$d \ln[\langle m^2 \rangle]_{av}/dK$	1.9626(13)	0.77	0.5128(22)	0.30	1.0664(30)	0.69#
Average	1.9548(38)		0.5151(19)		1.068 22(84)	
Weighted av.	1.957 58(59)		0.515 87(49)		1.067 98(86)	
Final	1.9576(13)		0.515 87(82)		1.0680(14)	
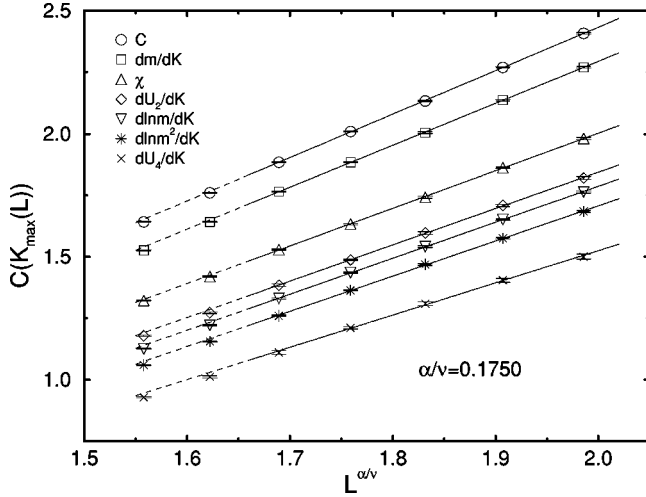
FIG. 5. FSS behavior of the specific heat, assuming $\alpha/\nu = 2/\nu - D = 0.1750$.

If hyperscaling is valid, the estimate (29) would imply $\gamma/\nu = D - 2\beta/\nu = 1.9683(17)$, which, however, turns out to be only barely consistent with the direct estimate (26) of γ/ν.

The FSS of $d[\langle|m|\rangle]_{\mathrm{av}}/dK$ is less well behaved. Here we had to discard for the K_{max_C}, $K_{\mathrm{max}_{dm/dK}}$, $K_{\mathrm{max}_{dlnm/dK}}$, and $K_{\mathrm{max}_{dlnm2/dK}}$ sequences both the $N = 2000$ and $N = 4000$ data in order to guarantee that all fits entering the average have a goodness-of-fit parameter $Q \geqslant 0.15$. We then obtain

$$(1 - \beta)/\nu = 1.0680 \pm 0.0014, \tag{31}$$

and by inserting the estimate (21) for $1/\nu$,

$$\beta/\nu = 0.5194 \pm 0.0026 \tag{32}$$

and

$$\beta = 0.3272 \pm 0.0014. \tag{33}$$

Recent MC estimates for regular SC lattices are $\beta/\nu = 0.518(7)$ in Ref. 68 and $\beta/\nu = 0.5185(15)$ in Ref. 69.

E. Critical exponent α

Due to the regular background term C_{reg} in the FSS behavior (14), the specific heat is usually among the most difficult quantities to analyze.[72] We tried nonlinear fits to the ansatz $C = C_{\mathrm{reg}} + aL^{\alpha/\nu}$, but for most sequences of pseudotransition points the errors in the parameters of this fit turned out to be large. We therefore fixed the exponent α/ν at the value one would expect if hyperscaling is valid,

$$\alpha/\nu = 2/\nu - D = 0.1750 \pm 0.0024, \tag{34}$$

$$\alpha = 2 - D\nu = 0.1102 \pm 0.0015, \tag{35}$$

and tested if linear two-parameter fits yield acceptable goodness-of-fit values. The results are shown in Fig. 5. We see that over the whole range of lattice sizes the expected linear behavior is satisfied. The quantitative analysis reveals some deviations for the two smallest lattice sizes, but for the
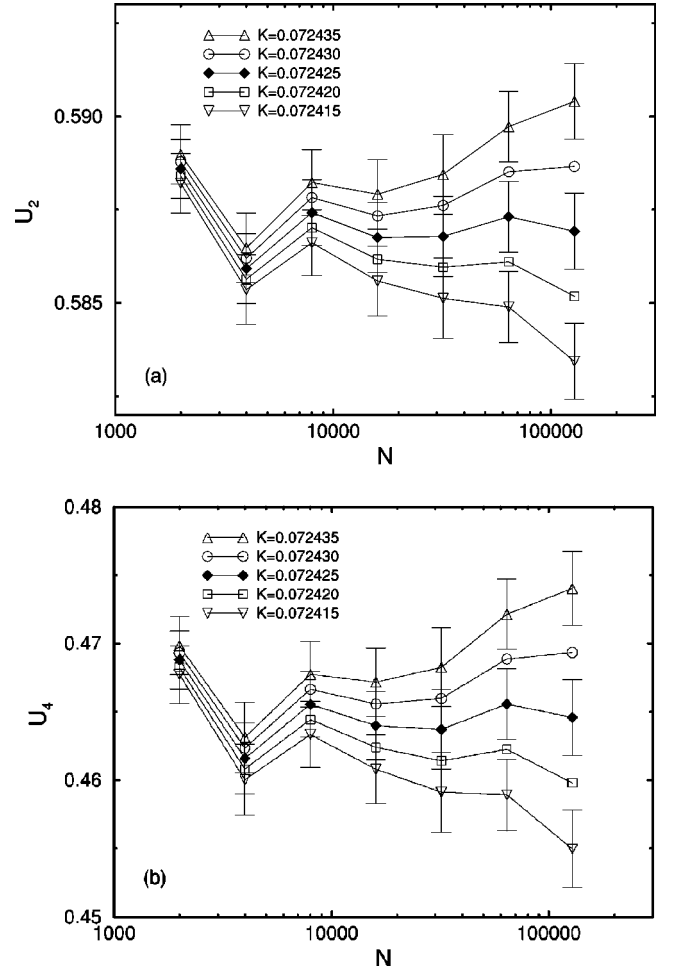

FIG. 6. FSS behavior of the magnetic cumulants. The central value of K is our best estimate (25) for the inverse critical temperature. For the neighboring curves the K values vary by about one statistical error bar.

fits starting with $N = 8000$ we obtained for all seven sequences of pseudotransition points goodness-of-fits parameters $Q \geqslant 0.5$.

F. Binder parameters U_2 and U_4

It is well known[73] that the $U_{2p}(K)$ curves for different lattice sizes L should intersect around (K_c, U_{2p}^*) with slopes $U_{2p}' \equiv dU_{2p}/dK \propto L^{1/\nu}$, where U_{2p}^* is the (weakly universal) "renormalized charge." In Fig. 6 we show U_2 and U_4 as a function of $N \equiv L^3$ for 5 K values around $K_c \approx 0.072\,425$. At our best estimate of K_c, both cumulants seem indeed to be almost independent of the lattice size. Taking as final estimate the weighted mean value (i.e., a least-squares fit to a constant) over the results for $N = 8000 – 128\,000$, we obtain

$$U_2^* = 0.58706 \pm 0.00044, \tag{36}$$

$$U_4^* = 0.4647 \pm 0.0012. \tag{37}$$

The variation due to the uncertainty in K_c is about twice the statistical error at fixed K (0.000 80 for U_2 and 0.0020 for

TABLE VIII. Recent estimates of critical parameters of the pure and disorderd 3D Ising model (SC = simple cubic lattice, LFT= lattice field theory, RG = renormalization group, SD = site-dilution, RIM = random Ising model).

Method	ν	γ/ν	U_4^*
SC[a]	0.6289(8)	1.970(14)	0.47
SC[b]	0.6301(8)	1.9630(30)	0.4652(4)
SC[c]	0.6294(5)[5]	1.9626(6)[6]	0.4656(4)[4]
SC ϕ^4 LFT[d]	0.6296(3)[4]	1.9642(4)[5]	0.465 55(9)
RG[e]	0.6304(13)	1.966(6)	–
This work	0.6299(5)	1.9576(13)	0.4647(12)
SD SC[f]	0.6837(24)[29]	1.9626(36)[9]	0.449(5)[2]
RIM-RG[g]	0.678(10)	1.970(3)	–
RIM-RG[h]	0.675	1.951	–

[a]Reference 68.
[b]Reference 69.
[c]Reference 67.
[d]Reference 71.
[e]Reference 15.
[f]Reference 6.
[g]Reference 13.
[h]Reference 11

U_4). For comparison, for the standard nearest-neighbor Ising model on a SC lattice, Ferrenberg and Landau[68] estimated $U_4^* \approx 0.47$, by combining results for three different spin models belonging to the Ising universality class Blöte et al.[69] derived $U_4^* = 0.4652(4)$, and Ballesteros et al.[67,70] obtained $U_4^* = 0.4656(4)[6]$. For the ϕ^4 lattice field theory Hasenbusch[71] extracted $U_4^* \approx 0.465\,55(9)$.

VI. CONCLUDING REMARKS

We have performed a detailed finite-size scaling analysis of single-cluster Monte Carlo simulations of the Ising model on three-dimensional Poissonian random lattices of Voronoi-Delaunay type. At first sight our use of different quantities to estimate the same critical exponent might appear redundant, since the various estimates are, of course, not independent in a statistical sense. Their consistency, however, gives confidence that corrections to the asymptotic scaling behavior are very small and can safely be neglected. Our estimates for the exponents ν, β/ν, and γ/ν are all consistent with the best numerical estimates for the three-dimensional Ising model and ϕ^4 field theory on regular lattices—at a very high level of accuracy which is comparable with the best estimates coming from field theoretical techniques; cf. Table VIII.[74] While our exponent ratio γ/ν would also be compatible with recent estimates for the 3D Ising disordered fixed point, our estimate for U_4^* is more consistent with the pure Ising model estimates. The cleanest result yields the critical exponent ν, where our result agrees within error bars with all previously derived estimates for the pure model but is clearly incompatible with the disordered fixed point value. We thus obtain strong evidence that, for the considered lattice sizes up to $N = 128\,000 \approx 50^3$, the Ising model on three-dimensional Poissonian random lattices of Voronoi-Delaunay type behaves effectively as on regular lattices.

Of course, we cannot exclude the possibility that on much

larger length scales (lattice sizes) the scaling behavior may change. Such a late crossover is conceivable in the case of weak disorder, where the asymptotic critical behavior governed by a "disordered" fixed point may show up only in the extremely close vicinity of criticality—that is, at extremely large system sizes in a finite-size scaling analysis. Even though the qualitative scaling behavior is expected to be universal, quantitative properties of the crossover point such as its location should depend on the strength of the disorder via nonuniversal amplitudes. In order to obtain for the random lattices a rough estimate of the strength $\mathcal{S}$ of the local connectivity disorder we have computed the relative variance of the local coordination numbers which may be viewed as a measure for the size of effective temperature variations over the lattice. From the probability density $P(q)$ displayed in Fig. 2 it is straightforward to obtain

$$\mathcal{S} \equiv \overline{(q-\bar{q})^2}/\bar{q}^2 = 0.0461, \tag{38}$$

with $\bar{q} = 2 + 48\pi^2/35 = 15.5354\ldots$. Similarly, for two-dimensional Poissonian Voronoi-Delaunay random lattices one finds $\mathcal{S} = 0.0491$ with $\bar{q} = 6$. The relative variance (38) can be compared with the fluctuations of the number B of active bonds per site in bond-diluted models. Here B follows a binomial distribution,

$$P(B) = \binom{2D}{B} p^B (1-p)^{2D-B},$$

where D is the dimension and p denotes the probability for a bond to be active (such that $p = 1$ corresponds to the pure model), and one obtains

$$\mathcal{S} = \overline{(B-\bar{B})^2}/\bar{B}^2 = \frac{1}{2D}\frac{1-p}{p}, \tag{39}$$

with $\bar{B} = 2Dp$. By equating Eqs. (38) and (39) and solving for the dilution parameter p one can thus determine an associated bond-dilution model with the same local disorder fluctuations as for the random lattices. For the three-dimensional case this yields $p = 0.7834$, and in two dimensions one finds $p = 0.8358$. In the terminology of three-dimensional bond-diluted Ising[7–9] and q-state Potts[17,19] models such a value of p belongs to the weak dilution regime where some influence of the disordered fixed point can be observed, but it is still difficult to clearly disentangle it. For site-diluted models the corresponding p value is presumably higher, in particular for weak dilution, since all bonds around a vacant site are nonactive. In the latter models, of course, the dilution parameter p can easily be tuned to study more accessible regions.

In view of the very high quality of our fits based on the leading FSS ansatz only we must conclude that in the case of Voronoi-Delaunay random lattices very much larger system sizes would be necessary to observe the expected crossover to the critical behavior associated with the disordered fixed point. This was clearly outside the scope of the present study and its computer budget which was equivalent to several years of fast workstation CPU time. Instead of further increasing the system size, an alternative and more promising

route for future studies could be a systematic variation of the random lattice construction by modifying the Poissonian nature of the site distribution such as to achieve larger values of $\mathcal{S}$ (corresponding to smaller values of p) or an investigation of the present random lattices coupled to a model with a larger critical exponent α where the expected crossover should set in for reasonable lattice sizes already for a moderate degree of local disorder.

APPENDIX: RANDOM LATTICE CONSTRUCTION

The employed algorithm for the random lattice construction works as follows. Adapting the method described in Ref. 60, we first draw randomly N sites uniformly distributed in a unit volume, thereby approximating a Poissonian distribution. For alternative distributions discussed in the literature see, e.g., Refs. 41 and 59. In the second step we link the sites according to the Voronoi-Delaunay prescription. We start by picking the first site that we drew and locate all its nearest neighbors, keeping them stored in an array. Then we proceed to the second site and search for all its nearest neighbors too; once finished with the second site we keep repeating the procedure until we have done it for all the sites. Of course, with this method we locate a given link twice, but the simplicity of its implementation pays off.

Starting from a given site, x_1, the linking procedure works as follows. Its nearest neighbor x_2 is located from within the few hundred sites forming, or belonging to, the "cloud of neighbors" around x_1. We will comment later the issue of how to determine a cloud of neighbors for a given site. Notice that some care must be exercised when approaching the boundaries of the lattice to ensure the periodic boundary conditions. Afterwards a third site x_3 is searched

for, and a triangle is constructed. In order to locate this third site, we draw circumferences going through x_1, x_2, and the few hundred sites belonging to the cloud of neighbors of x_1. We pick as x_3 the site for which the radius of the circumference is the smallest. From the triangle $\triangle(x_1, x_2, x_3)$ we proceed to locate a fourth site x_4 linked to x_1 and build a tetrahedron $\tau(x_1, x_2, x_3, x_4)$. When a triangle still has not been used to build a tetrahedron from it, it is termed "active" and a logical flag is turned "on." When already used, it is renamed to "inactive" and the flag is turned "off."

To construct a tetrahedron from a triangle we split the volume in two half spaces: one "above" and the other "below" the plane lying on the triangle $\triangle(x_1, x_2, x_3)$. Let us suppose that we search for x_4 in the half space "above" the triangle. In order to determine x_4, we draw spheres going through x_1, x_2, x_3 and the sites belonging to the cloud of neighbors of x_1 placed in the half space in which we are working. If we happen to find several trial sites for which their distance to the circumcenter of the triangle $\triangle(x_1, x_2, x_3)$ is smaller than the radius of the circumscribed circle of $\triangle(x_1, x_2, x_3)$, then we pick as x_4 the site for which the radius of the circumscribed sphere of $\tau(x_1, x_2, x_3, x_4)$ is the biggest. If, on the contrary, all the trial sites lie at a distance from the circumcenter of the triangle $\triangle(x_1, x_2, x_3)$ greater than the radius of the circumscribed circle of $\triangle(x_1, x_2, x_3)$, then we pick as x_4 the site for which the radius of the circumscribed sphere of $\tau(x_1, x_2, x_3, x_4)$ is the smallest. From the newly built tetrahedron $\tau(x_1, x_2, x_3, x_4)$, we can take two "active" triangles $\triangle(x_1, x_2, x_4)$ and $\triangle(x_1, x_3, x_4)$ to continue building tetrahedra from triangles and then triangles from tetrahedra. The closer neighbors of a given site x_1 are all found when there is no "active" triangle left connected to the site.

When describing how to locate x_1's nearest neighbor x_2 or how to find x_3 afterwards we emphasized that we only search from within the sites forming a cloud of neighbors around x_1. Its meaning is that *before* starting the linking procedure we set up an array for each site in the lattice containing the sites forming its cloud. A given site will belong to the cloud of, say, x_1 if it lies within a sphere centered in x_1. The radius of the sphere is chosen such that, on the average, the number of sites within the sphere is 3 times of an *a priori* upper limit to the maximum number of links that a site is likely to have in a finite Voronoi-Delaunay random lattice. To implement an efficient search of the sites which will belong to the cloud of neighbors of a given site, we subdivided the unit volume into smaller boxes. The optimal box size should be large enough to ensure that nearest neighbors will be located in the same box or at least in one of the 26 surrounding boxes, but small enough to minimize the time needed for testing all trial sites in a box.

---

[1] A.B. Harris, J. Phys. C **7**, 1671 (1974).

[2] J. Chayes, L. Chayes, D.S. Fisher, and T. Spencer, Phys. Rev. Lett. **57**, 2999 (1986).

[3] Y. Imry and M. Wortis, Phys. Rev. B **19**, 3580 (1979); A.N. Berker, *ibid.* **29**, 5243 (1984); K. Hui and A.N. Berker, Phys. Rev. Lett. **62**, 2507 (1989); **63**, 2433(E) (1989); A. Aizenman

and J. Wehr, *ibid.* **62**, 2503 (1989); A.N. Berker and K. Hui, in *Science and Technology of Nanostructured Magnetic Materials*, edited by G.C. Hadjipanayis, G. Prinz, and L. Paretti (Plenum, New York, 1991).

[4] H.-O. Heuer, Europhys. Lett. **12**, 551 (1990); Phys. Rev. B **42**, 6476 (1990); J.-S. Wang, M. Wöhlert, H. Mühlenbein, and D.

Chowdhury, Physica A **166**, 173 (1990); T. Holey and M. Fähnle, Phys. Rev. B **41**, 11 709 (1990).

[5] S. Wiseman and E. Domany, Phys. Rev. Lett. **81**, 22 (1998); Phys. Rev. E **58**, 2938 (1998).

[6] H.G. Ballesteros, L.A. Fernández, V. Martín-Mayor, A. Muñoz Sudupe, G. Parisi, and J.J. Ruiz-Lorenzo, Phys. Rev. B **58**, 2740 (1998).

[7] P.-E. Berche, C. Chatelain, B. Berche, and W. Janke, Comput. Phys. Commun. **147**, 427 (2002).

[8] P.-E. Berche, C. Chatelain, B. Berche, and W. Janke, in *High Performance Computing in Science and Engineering in Munich 2002* (Springer, Berlin, in press).

[9] M. Hellmund and W. Janke, Comput. Phys. Commun. **147**, 435 (2002).

[10] K.B. Varnashev, Phys. Rev. B **61**, 14 660 (2000).

[11] R. Folk, Yu. Holovatch, and T. Yavors'kii, Phys. Rev. B **61**, 15 114 (2000).

[12] D.V. Pakhnin and A.I. Sokolov, Phys. Rev. B **61**, 15 130 (2000).

[13] A. Pelissetto and E. Vicari, Phys. Rev. B **62**, 6393 (2000).

[14] R. Folk, Yu. Holovatch, and T. Yavors'kii, cond-mat/0106468 (unpublished).

[15] R. Guida and J. Zinn-Justin, J. Phys. A **31**, 8103 (1998).

[16] H.G. Ballesteros, L.A. Fernández, V. Martín-Mayor, A. Muñoz Sudupe, G. Parisi, and J.J. Ruiz-Lorenzo, Phys. Rev. B **61**, 3215 (2000).

[17] C. Chatelain, B. Berche, W. Janke, and P.E. Berche, Phys. Rev. E **64**, 036120 (2001).

[18] C. Chatelain, P.-E. Berche, B. Berche, and W. Janke, Nucl. Phys. B (Proc. Suppl.) **106&107**, 899 (2002); Comput. Phys. Commun. **147**, 431 (2002).

[19] M. Hellmund and W. Janke, Nucl. Phys. B (Proc. Suppl.) **106-107**, 923 (2002).

[20] D. Matthews-Morgan, D.P. Landau, and R.H. Swendsen, Phys. Rev. Lett. **53**, 679 (1984).

[21] M.A. Novotny and D.P. Landau, J. Magn. Magn. Mater. **15-18**, 247 (1980); Phys. Rev. B **24**, 1468 (1981); M.A. Novotny, D.P. Landau, and R.H. Swendsen, *ibid.* **32**, 3112 (1985).

[22] G. Jug and B.N. Shalaev, Phys. Rev. B **54**, 3442 (1996); M. Picco, *ibid.* **54**, 14 930 (1996); J. Cardy and J.L. Jacobsen, Phys. Rev. Lett. **79**, 4063 (1997).

[23] S. Wiseman and E. Domany, Phys. Rev. E **51**, 3074 (1995); **52**, 3469 (1995).

[24] For a review, see W. Selke, L.N. Shchur, and A.L. Talapov, in *Annual Reviews of Computational Physics I*, edited by D. Stauffer (World Scientific, Singapore, 1994), p. 17.

[25] Vik.S. Dotsenko and Vl.S. Dotsenko, JETP Lett. **33**, 37 (1981); Adv. Phys. **32**, 129 (1983).

[26] B.N. Shalaev, Sov. Phys. Solid State **26**, 1811 (1984); Phys. Rep. **237**, 129 (1994); R. Shankar, Phys. Rev. Lett. **58**, 2466 (1987); **61**, 2390 (1988); A.W.W. Ludwig, *ibid.* **61**, 2388 (1988); Nucl. Phys. B **330**, 639 (1990).

[27] V.B. Andreichenko, Vl.S. Dotsenko, W. Selke, and J.-S. Wang, Nucl. Phys. B **344**, 531 (1990); J.-S. Wang, W. Selke, Vl.S. Dotsenko, and V.B. Andreichenko, Europhys. Lett. **11**, 301 (1990); Physica A **164**, 221 (1990); A.L. Talapov and L.N. Shchur, J. Phys.: Condens. Matter **6**, 8295 (1994); F.D.A. Aarão Reis, S.L.A. de Queiroz, and R.R. dos Santos, Phys. Rev. B **56**, 6013 (1997); D. Stauffer, F.D.A. Aarão Reis, S.L.A. de Queiroz, and R.R. dos Santos, Int. J. Mod. Phys. C **8**, 1209 (1997).

[28] A. Roder, J. Adler, and W. Janke, Phys. Rev. Lett. **80**, 4697 (1998); Physica A **265**, 28 (1999).

[29] S. Chen, A.M. Ferrenberg, and D.P. Landau, Phys. Rev. Lett. **69**, 1213 (1992); Phys. Rev. E **52**, 1377 (1995).

[30] F. Yasar, Y. Gündüc, and T. Celik, Phys. Rev. E **58**, 4210 (1998); Physica A **274**, 537 (1999).

[31] C. Chatelain and B. Berche, Phys. Rev. Lett. **80**, 1670 (1998).

[32] A. Roder and W. Janke (unpublished).

[33] B. Berche and C. Chatelain, cond-mat/0207421 (unpublished).

[34] J.L. Meijering, Philips Res. Rep. **8**, 270 (1953).

[35] R. Collins, Proc. Phys. Soc. **1**, 1461 (1968); in *Phase Transitions and Critical Phenomena*, edited by C. Domb and M.S. Green (Academic Press, London, 1972), p. 271.

[36] J.M. Ziman, *Models of Disorder* (Cambridge University Press, Cambridge, England, 1976).

[37] C. Itzykson and J.-M. Drouffe, *Statistical Field Theory* (Cambridge University Press, Cambridge, England, 1989), Vol. 2.

[38] N.H. Christ, R. Friedberg, and T.D. Lee, Nucl. Phys. B **202**, 89 (1982); Nucl. Phys. B: Field Theory Stat. Syst. **B210** [FS6], 310 (1982); **B210** [FS6], 337 (1982).

[39] C. Holm and W. Janke, Phys. Lett. B **390**, 59 (1997).

[40] C. Holm and W. Janke, Int. J. Mod. Phys. A **14**, 3885 (1999).

[41] C. Moukarzel and H.J. Herrmann, J. Stat. Phys. **68**, 911 (1992).

[42] H. Puhl, Physica A **197**, 14 (1993).

[43] F. David and J.-M. Drouffe, Nucl. Phys. B (Proc. Suppl.) **4**, 83 (1988).

[44] C. Itzykson, in *Progress in Gauge Field Theories*, Cargése Summer School proceedings, edited by G. t Hooft (Plenum Press, New York, 1983).

[45] R. Friedberg and H.-C. Ren, Nucl. Phys. B: Field Theory Stat. Syst. **B235** [FS11], 310 (1984); H.-C. Ren, *ibid.* **B235** [FS11], 321 (1984).

[46] K. Binder, in *Phase Transitions and Critical Phenomena*, edited by C. Domb and M.S. Green (Academic, New York, 1976), vol. 5B, p. 1; in *Monte Carlo Methods in Statistical Physics*, edited by K. Binder (Springer, New York, 1979), p. 1; M. E. Barber, in *Phase Transitions and Critical Phenomena*, edited by C. Domb and J.L. Lebowitz (Academic, New York, 1983) vol. 8, p. 145; see also the articles in *Finite-Size Scaling and Numerical Simulations of Statistical Systems*, edited by V. Privman (World Scientific, Singapore, 1990).

[47] U. Wolff, Phys. Rev. Lett. **62**, 361 (1989); Nucl. Phys. B **334**, 581 (1990).

[48] R.H. Swendsen and J.-S. Wang, Phys. Rev. Lett. **58**, 86 (1987); J.-S. Wang and R.H. Swendsen, Physica A **167**, 565 (1990).

[49] A.M. Ferrenberg and R.H. Swendsen, Phys. Rev. Lett. **61**, 2635 (1988); **63**, 1658(E) (1989).

[50] C.F. Baillie, K.A. Hawick, and D.A. Johnston, Phys. Lett. B **328**, 284 (1994).

[51] K. Anagnostopoulos, P. Bialas, and G. Thorleifsson, J. Stat. Phys. **94**, 321 (1999).

[52] W. Janke and D.A. Johnston, Phys. Lett. B **460**, 271 (1999); Nucl. Phys. B: Field Theory Stat. Syst. **B578** [FS], 681 (2000); J. Phys. A **33**, 2653 (2000).

[53] C.F. Baillie, W. Janke, and D.A. Johnston, Phys. Lett. B **388**, 14 (1996); Nucl. Phys. B (Proc. Suppl.) **53**, 732 (1997).

[54] D. Espriu, M. Gross, P.E.L. Rakow, and J.F. Wheater, Nucl. Phys. B: Field Theory Stat. Syst. **B265** [FS15], 92 (1986).

[55] W. Janke, M. Katoot, and R. Villanova, Phys. Lett. B **315**, 412

(1993); Nucl. Phys. B (Proc. Suppl.) **34**, 698 (1994); Phys. Rev. B **49**, 9644 (1994).

[56] W. Janke and R. Villanova, Phys. Lett. A **209**, 179 (1995); Nucl. Phys. B (Proc. Suppl.) **47**, 641 (1996).

[57] J. Ambjørn, K.N. Anagnostopoulos, T. Ichihara, L. Jensen, and Y. Watabiki, J. High Energy Phys. **11**, 022 (1998); J. Ambjørn, K.N. Anagnostopoulos, and G. Thorleifsson, Nucl. Phys. B (Proc. Suppl.) **63**, 742 (1998); J. Ambjørn and K.N. Anagnostopoulos, Nucl. Phys. B **497**, 445 (1997); M. Bowick, V. John, and G. Thorleifsson, Phys. Lett. B **403**, 197 (1997).

[58] P.E. Berche, C. Chatelain, and B. Berche, Phys. Rev. Lett. **80**, 297 (1998).

[59] G. Le Caër and J.S. Ho, J. Phys. A **23**, 3279 (1990).

[60] M. Tanemura, T. Ogawa, and N. Ogita, J. Comput. Phys. **51**, 191 (1983).

[61] U. Wolff, Phys. Lett. B **228**, 379 (1989).

[62] C.F. Baillie and P.D. Coddington, Phys. Rev. B **43**, 10617 (1991).

[63] P. Tamayo, R.C. Brower, and W. Klein, J. Stat. Phys. **58**, 1083 (1990); J.-S. Wang, Physica A **164**, 240 (1990); M. Hasenbusch and S. Meyer, Phys. Lett. B **241**, 238 (1990); W. Janke, Phys. Lett. A **148**, 306 (1990).

[64] W. Janke, in *Proceedings of the Euro Winter School Quantum Simulations of Complex Many-Body Systems: From Theory to Algorithms*, edited by J. Grotendorst, D. Marx, and A. Muramatsu (John von Neumann Institute for Computing, Jülich, 2002), NIC Series, vol. 10, pp. 423–445; in *Computational Physics: Selected Methods—Simple Exercises—Serious Applications*, edited by K.H. Hoffmann and M. Schreiber (Springer, Berlin, 1996), p. 10; R.H. Swendsen, J.-S. Wang, and A.M. Ferrenberg, in *The Monte Carlo Method in Condensed Matter Physics*, edited by K. Binder (Springer, Berlin, 1991); C.F. Baillie,

[65] Int. J. Mod. Phys. C **1**, 91 (1990); A.D. Sokal, in *Quantum Fields on the Computer*, edited by M. Creutz (World Scientific, Singapore, 1992); see also *Monte Carlo Methods in Statistical Mechanics: Foundations and New Algorithms*, lecture notes, Cours de Troisième Cycle de la Physique en Suisse Romande, Lausanne, 1989; N. Madras and A.D. Sokal, J. Stat. Phys. **50**, 109 (1988).

[65] R.G. Miller, Biometrika **61**, 1 (1974); B. Efron, *The Jackknife, the Bootstrap and other Resampling Plans* (SIAM, Philadelphia, PA, 1982).

[66] W.H. Press, S.A. Teukolsky, W.T. Vetterling, and B.P. Flannery, *Numerical Recipes in Fortran 77—The Art of Scientific Computing*, second corrected edition (Cambridge University Press, Cambridge, England, 1996).

[67] H.G. Ballesteros, L.A. Fernández, V. Martín-Mayor, A. Muñoz Sudupe, G. Parisi, and J.J. Ruiz-Lorenzo, J. Phys. A **32**, 1 (1999).

[68] A.M. Ferrenberg and D.P. Landau, Phys. Rev. B **44**, 5081 (1991).

[69] H.W.J. Blöte, E. Luijten, and J.R. Heringa, J. Phys. A **28**, 6285 (1995).

[70] In Refs. 67 and 71 the error bars are given separately for purely statistical and more systematic errors indicated by "(. . .)" and "[. . .]," respectively.

[71] M. Hasenbusch, J. Phys. A **32**, 4851 (1999).

[72] C. Holm and W. Janke, Phys. Rev. Lett. **78**, 2265 (1997).

[73] K. Binder, Z. Phys. B: Condens. Matter **43**, 119 (1981).

[74] In the summarizing Table VIII we confine ourselves to those critical parameters which are usually measured or calculated independently. Other exponents are often derived by scaling or hyperscaling relations which does not add any new information.